Original Research

Machine Learning Prediction of Optical Band Gap in In-Se Chalcogenide Thin Films

Madhvi Bhardwaj [1], Lakshay Dhiman [1], Rita Sharma [1,*]

[1] Department of Physics, University School of Sciences, Rayat Bahra University, Mohali, Punjab 140104, India.
* Correspondence: reetasharma2012@gmail.com

Received: March 15, 2026; Accepted: April 13, 2026

Abstract: Machine learning provides a powerful approach for predicting material properties from existing experimental data. In this study, the optical band gap of In–Se chalcogenide thin films was predicted using a literature-derived dataset containing film thickness, indium composition, and selenium composition. A Random Forest regression model was developed to capture the nonlinear relationship between these parameters and the optical band gap. The model demonstrates strong predictive performance with a coefficient of determination (R^2 = 0.929) and a root mean square error (RMSE = 0.071 eV), indicating close agreement between predicted and reported band gap values. Feature-importance analysis reveals that film thickness is the dominant predictor, contributing about 63% of the total model importance, followed by selenium and indium composition. The observed dependence reflects underlying physical effects such as thickness-related electronic confinement and compositional variations that influence the electronic structure of In–Se thin films. These results demonstrate that literature-driven machine learning can provide rapid and reliable estimation of optical band gaps, offering an efficient strategy for guiding the design of chalcogenide thin films with targeted optoelectronic properties.

Keywords: In-Se chalcogenide; composition; thickness; optical band gap; machine learning.

1. Introduction

Selenium-based chalcogenide materials exhibit high absorption, tunable band gaps, and layered structures, making them suitable for optoelectronic devices such as photovoltaics, photodetectors, and memory applications. Undoped selenium thin films have been widely studied for their photoconductive properties and stability, while doped selenium-based chalcogenide systems often exhibit enhanced electrical conductivity, improved carrier transport, and tunable optical properties. These characteristics make Se-based thin films particularly attractive for applications in optical switching devices, phase-change memory, infrared detectors, and thin-film photovoltaic devices. In particular, thin films of In–Se compositions, including stoichiometric In_2Se_3 and slightly non-stoichiometric variants (In_XSe_Y), have drawn attention due to their optical band gap sensitivity to film thickness, composition, crystal structure, and growth conditions [1-2].

Physical vapour deposition methods provide precise control over film thickness and uniformity, resulting in well-defined optical characteristics. Studies have shown that In-Se films grown by thermal evaporation exhibit multiple crystalline phases (α, β, γ), and the phase formed depends strongly on substrate temperature, deposition rate, and post-growth annealing [3]. The optical band gap of these films ranges widely, typically from ~1.39 eV to ~2.09 eV, depending on structural phase and thickness [4]. Even slight variations in composition can shift the band gap, highlighting the interplay between stoichiometry and optical properties [5]. These variations are generally attributed to changes in electronic structure, quantum confinement effects in thin films, and defect-related states that influence the optical absorption edge. In our previous work, irradiation effects on selenium-based chalcogenide thin films were shown to significantly influence their structural and optical properties [6-7].

Several experimental studies have reported that the optical band gap of In_2Se_3 thin films varies significantly depending on structural phase, deposition technique, and film thickness. These variations arise due to differences in atomic ordering, grain size, and defect density that influence the electronic structure of the films [8-11]. Moreover, deposition parameters such as substrate temperature, evaporation rate, and post-deposition annealing have been shown to strongly affect both the structural and optical properties of In–Se thin films. Understanding these relationships is therefore essential for optimizing chalcogenide thin films for optoelectronic applications.

Despite these extensive studies, establishing systematic relationships between thickness, composition, and optical band gap remains challenging. Traditional approaches require fabricating and measuring multiple samples under different conditions, which is time-consuming and resource-intensive. In this context, machine learning (ML) offers a promising alternative, enabling the prediction of optical properties from existing experimental data without performing additional experiments [12-14].

In the present work, we compiled a dataset of In–Se thin films from the literature, focusing on samples prepared by thermal evaporation and other physical vapour deposition techniques. For each sample, we extracted thickness, composition, and optical band gaps. Using regression-based ML models, the optical band gap is predicted as a function of these descriptors, demonstrating the potential of data-driven approaches for the design of In–Se thin films with tailored optical properties [15]. This framework provides a fast and efficient tool for exploring the effect of thickness and compositional variations on band gaps without performing extensive laboratory experiments.

The novelty of this work lies in the combination of literature-derived experimental data with machine learning techniques to analyze the dependence of the optical band gap of In–Se thin films on thickness and composition. The scope of this work is therefore to provide a predictive framework for understanding band gap variation in In–Se chalcogenide thin films and to highlight the potential of machine learning in accelerating materials analysis and design.

2. Materials and methods

In this work, a machine learning approach was employed to predict the optical band gap of In-Se thin films using experimentally reported thickness and composition data collected from the literature. Since the present study is based on literature-derived experimental data, the structural and optical characterization of the thin films (including thickness measurement and optical band gap determination) were performed in the original experimental studies from which the dataset was compiled.

The predicted task was formulated as a supervised nonlinear regression problem aimed at learning the functional relationship between film parameters and the corresponding band gap. The objective is to approximate the functional relationship between experimentally measured thickness, composition, and the corresponding band gap. For each sample, the input feature vector was defined as:

$$X = [t, C_{In}, C_{Se}] \quad (1)$$

Where t denotes the film thickness in nanometers (nm), C_{In} represents the atomic percentage of indium, and C_{Se} represents the atomic percentage of selenium. The target variable y corresponds to the experimentally reported optical band gap, expressed in electron volts (eV). Although indium and selenium atomic percentages are complementary in ideal stoichiometric compositions (CSe ≈ 100 − CIn), both variables were retained in the feature set. Literature-reported compositions often exhibit small deviations due to measurement uncertainty, rounding, and differing reporting conventions (nominal vs measured composition).

Inclusion of both compositional descriptors therefore preserves reported stoichiometric variability and was found to improve model prediction accuracy.

The nonlinear regression problem can therefore be expressed as:

$$y = f(X) \tag{2}$$

Where f represents a nonlinear mapping learned using an ensemble-based machine learning model.

2.1. Dataset description

The dataset was compiled from previously published experimental studies on In-Se thin films prepared using physical vapour deposition techniques [16-32]. To maintain consistency in fabrication conditions and reduce variability caused by different synthesis routes, only In–Se thin films prepared using physical vapour deposition techniques reported in the literature were included in the dataset. The compiled dataset contained 42 samples with variables such as thickness, composition of In and Se in In-Se chalcogenide thin films, and band gap. The thickness of the films reported in the dataset ranges approximately from 100 nm to 1000 nm depending on the deposition conditions used in the original experimental studies. The optical band gap values were obtained from optical absorption measurements and estimated using the Tauc relation as reported in the corresponding references.

2.2. Machine learning model and training procedure

The observed nonlinear dependence of band gap on thickness and composition motivates the use of a nonlinear regression model capable of capturing coupled thickness–compositional effects. The model used in this study is the Random Forest regression model [19]. Random Forest is a non-parametric ensemble learning method that constructs multiple decision trees using bootstrap sampling of the training data and random feature selection at each split. Ensemble tree-based models are particularly well suited for small, nonlinear materials datasets derived from heterogeneous literature sources. This stochastic approach helps prevent overfitting and improves the model’s ability to generalize to new data. The final prediction is obtained by averaging the outputs of all individual decision trees:

$$\hat{y} = \frac{1}{T}\sum_{k=1}^{T} f_k\,(X) \tag{3}$$

Where T denotes the total number of trees and f_k represents the prediction from the k-th tree. The model hyperparameters were selected to control complexity while maintaining sufficient flexibility. The number of trees (n_estimators) was set to 300 to ensure stable ensemble averaging. The maximum depth of each tree (max_depth) was limited to 5 to prevent excessive model complexity. The minimum number of samples required at each leaf node (min_samples_leaf) was set to 2 to avoid leaves based on single observations. The random seed was fixed at 42 to ensure reproducibility.

Model performance was evaluated using 5 fold cross validation with shuffling and a fixed random seed. The dataset was divided into five approximately equal subsets. In each iteration, four folds were used for training and one fold for validation. This process was repeated five times so that each fold served once as the validation set. Final performance metrics were computed as the average across all folds.

2.3. Model evaluation metrics

The predictive performance of the model was assessed using two complementary regression metrics:

2.3.1. Coefficient of determination (R^2)

R^2 measures the proportion of variance in the experimental band gap values explained by the model.

$$R^2 = 1 - \frac{\sum_{i=1}^{n}(y_i-\hat{y}_i)^2}{\sum_{i=1}^{n}(y_i-\bar{y})^2} \tag{4}$$

2.3.2. Root mean square error (RMSE)

RMSE measures the standard deviation of prediction errors between experimental and predicted band gap values and provides an error estimate in the same units as the target variable (eV). It is defined as:

$$RMSE = \left(\frac{1}{n}\sum_{i=1}^{n} (y_i - \hat{y}_i)^2\right)^{1/2} \quad (5)$$

where y_i represents the experimentally reported band gap, $\hat{y}_i$ denotes the model-predicted band gap, and n is the total number of samples. Lower RMSE values indicate better agreement between predicted and experimental values.

3. Results and discussion

The extracted experimental data, compiled from previously reported experimental studies on In–Se thin films prepared using physical vapour deposition techniques[16-32], show the dependence of optical band gap on film thickness and elemental composition (Figure 1).

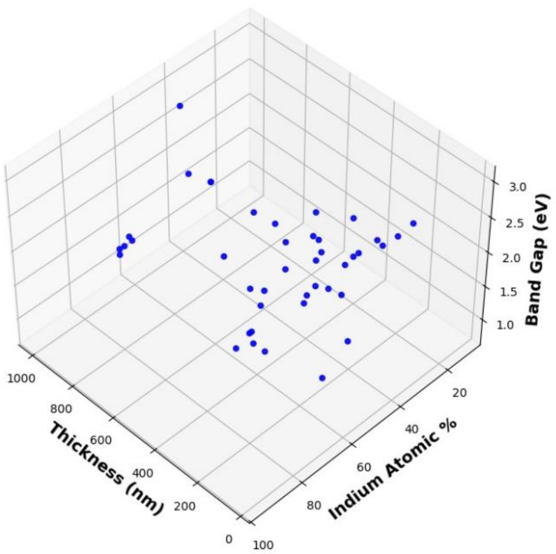

Figure 1. Three-dimensional visualization of the dependence of optical band gap on film thickness and composition for In-Se thin films.

This distribution shows that band gap variation depends on the combined influence of thickness and composition, with no single parameter independently controlling the electronic behavior. Since selenium composition is complementary to indium, both variables represent the same compositional degree of freedom; they are shown together to preserve reported stoichiometric information from literature.

3.1. Feature importance analysis

Feature importance was computed using the impurity-based importance measure inherent to the Random Forest algorithm. The normalized importance values of thickness, Selenium composition, and Indium composition obtained from the trained model are 0.632, 0.209, and 0.159 respectively. Film thickness contributes approximately 63% of the total predictive importance. This dominance of thickness likely reflects quantum confinement and structural phase evolution effects reported in In-Se thin films [33]. Selenium composition contributes about 21%, while indium composition contributes approximately 16%. The distribution of importance values suggests that both thickness and compositional factors influence the band gap. Thickness likely affects electronic properties through mechanisms such as quantum confinement, defect density variation, strain, and crystallinity changes. Meanwhile, deviations in stoichiometry can modify defect states and electronic structure, contributing to observable band gap variation. It is important to note that impurity-based feature importance reflects the statistical contribution of each feature to variance reduction within the ensemble model and does not establish direct physical causation [12-14].

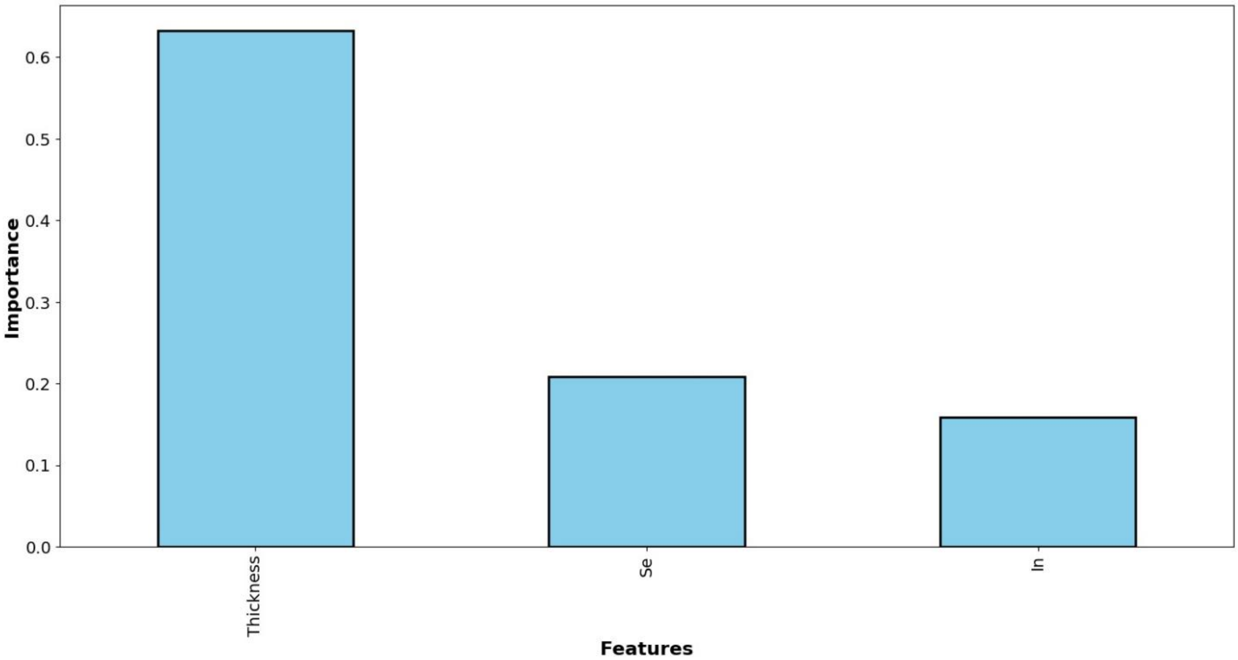

Figure 2. Feature importance from the Random Forest regression model for band gap prediction of In-Se thin films. Thickness shows the highest contribution, followed by elemental composition variables.

The obtained machine learning results can also be interpreted from the known physical behaviour of chalcogenide thin films. In In–Se systems, the optical band gap is strongly influenced by structural and compositional parameters. Variations in film thickness can modify the optical band gap due to changes in structural ordering, grain size, and defect density, which influence the electronic structure and optical absorption edge of the material. In very thin films, additional effects such as quantum confinement may also contribute to band gap variation. Similarly, changes in indium and selenium composition alter the stoichiometry of the In–Se network, affecting bonding configurations and the distribution of electronic states near the band edges. The feature importance analysis obtained from the Random Forest model indicates that film thickness has the strongest influence on band gap variation in the studied dataset, while compositional parameters provide secondary contributions. This observation is consistent with experimental reports on thickness-dependent optical properties of In–Se chalcogenide thin films. Similar thickness-dependent optical band gap variations have also been reported in recent experimental studies on In-Se thin films [30, 33, 36]

Table 1. Experimental and predicted band gap values used for model testing.

Thickness (nm)	In (%)	Se (%)	Band Gap (eV)	Predicted Band Gap (eV)
200	40	60	2.35	2.33
20	59.2	40.8	2.60	2.70
140	50	50	1.89	1.81
276	40	60	2.10	2.06

Figure 3 shows that the predicted values closely follow the experimental trend for all samples, indicating that the model successfully captures the dominant relationship between the input features and band gap.

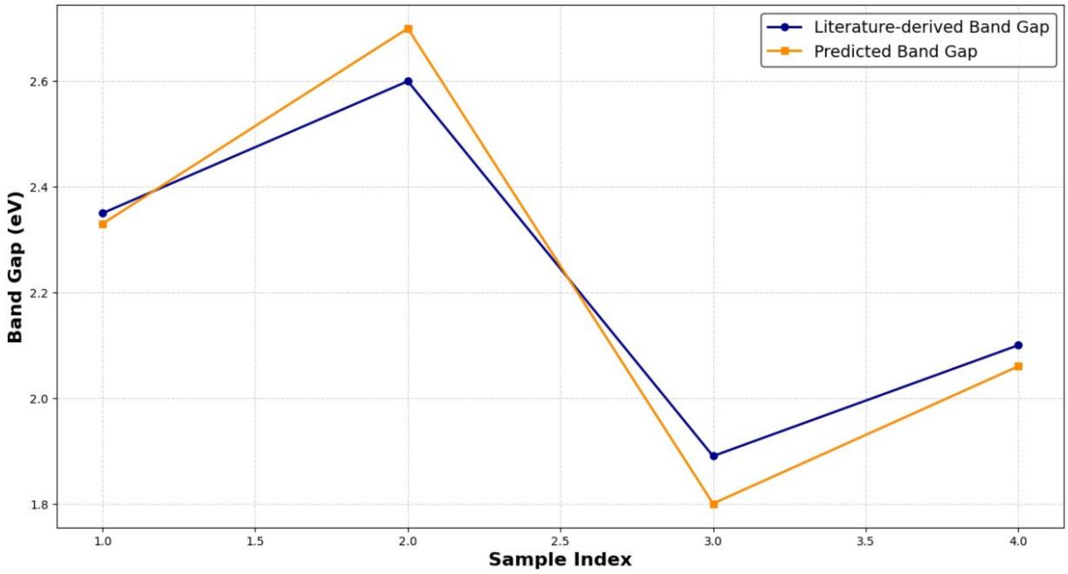

Figure 3. Comparison between literature-derived and ML–predicted band gap values for selected In–Se thin film samples, showing strong agreement with high R^2 and low prediction error.

The coefficient of determination R^2 is 0.929 which confirms that approximately 93% of the variance in the experimental band gap values is explained by the model. The RMSE value of 0.071 eV indicates low dispersion between predicted and experimental band gap values. This error magnitude is comparable to typical experimental uncertainties in optical band gap estimation using Tauc analysis [36-37].

Small deviations appear for some samples, particularly at lower band gap values; however, the overall agreement between predicted and literature values remains strong. This confirms that the regression model can reliably estimate band gaps within the studied range when thickness and composition inputs are properly represented.

4. Conclusions

In this study, the optical band gap of In–Se thin films was investigated as a function of composition and thickness using experimental literature data combined with a Random Forest regression model based on machine-learning. The comparison between literature-derived and predicted band gap values demonstrates strong predictive capability, with a coefficient of determination $R^2 = 0.929$ and a root mean square error RMSE = 0.071 eV. These results indicate that the model successfully captures the relationship between film parameters and optical band gap. The predicted band gap trends are consistent with experimentally reported thickness- and composition-dependent optical behaviour of In–Se chalcogenide thin films. The feature importance analysis further reveals that film thickness has a dominant influence on the band gap compared with compositional variations within the studied range. The proposed approach demonstrates that reliable prediction of optical properties can be achieved using literature-derived datasets, providing a useful framework for accelerated materials analysis and guiding future experimental design. Future studies may extend this data-driven methodology to larger datasets and more complex chalcogenide systems, including ternary and quaternary compositions, as well as to other material characteristics such as structural, electrical, and photovoltaic properties of thin films.

Declarations

Availability of data and material: The datasets used and analyzed during the current study are available from the corresponding author on reasonable request.

Author contributions: Madhvi Bhardwaj conceived and designed the research framework and prepared the initial draft of the manuscript; Lakshay Dhiman carried out the computational work; Rita Sharma supervised the work and provided critical guidance on the analytical methods and interpretation of results. All authors have read and approved the final manuscript. All authors contributed to editorial changes in the manuscript. All authors have participated sufficiently in the work and agreed to be accountable for all aspects of the work.

Acknowledgments: The authors acknowledge the support and encouragement provided by the institution.

Funding: This research received no external funding.

Conflicts of interest: The authors declare no conflict of interest.

References

1. Bindu, K.; Kartha, C.S.; Vijayakumar, K.P.; Abe, T.; Kashiwaba, Y. Structural, optical and electrical properties of In_2Se_3 thin films formed by annealing chemically deposited Se and vacuum-evaporated In stack layers. *Applied Surface Science* 2002, 191(1-4), 138–147. https://doi.org/10.1016/S0169-4332(02)00172-1
2. Patel, P.; Patel, V.; Vyas, S.; Patel, J.; Pavagadhi, H. Optical investigations of $In_2Se_{2.7}Sb_{0.3}$ thin films prepared by thermal evaporation technique. *Materials Science Forum* 2019, 969, 355 – 360. https://doi.org/10.4028/www.scientific.net/MSF.969.355
3. Qasrawi, J.F. Temperature dependence of the direct allowed transitions band gap and optical constants of polycrystalline α-In_2Se_3 thin films. *Thin Solid Films* 2006, 514(1-2), 267 – 271. https://doi.org/10.1016/j.tsf.2006.02.028
4. Ebraheem, B.; Farag, A.A.M.; Ashour, A.H.; Roushdy, N.; El-Nahass, M.M. Enhancement of optical absorption and dispersion characteristics of nanocrystalline In_2Se_3 films: Impact of γ-ray irradiation. *Journal of Materials Science: Materials in Electronics* 2023, 34, 382. https://doi.org/10.1007/s10854-022-09776-4
5. Petritz, R.L. Electrical and optical properties of In_2Se_3 thin films. *Thin Solid Films* 1986, 137(1), 27–37. https://doi.org/10.1016/0040-6090(86)90191-4
6. Sharma, R.; Sharma, S.; Sharma, P.K.; Thangaraj, R.; Singh, S.; Goswamy, J.K. Experimental and theoretical investigations for gamma-irradiation effects in Se-rich $Ag_{10}Sb_{20}Se_{70}$ thin films. *Journal of Materials Science: Materials in Electronics* 2025, 36, 1644. https://doi.org/10.1007/s10854-025-15702-1
7. Sharma, S.; Sharma, R.; Kumar, P.; Thangaraj, R.; Asokan, K.; Mian, M. Effect of gamma irradiation on structure and photoconductivity of amorphous $Sb_{30}Se_{70}$ chalcogenide films. *Journal of Non-Crystalline Solids* 2020, 530, 119807. https://doi.org/10.1016/j.jnoncrysol.2019.119807
8. Ebraheem, B.; Farag, A.A.M.; Ashour, A.H.; Roushdy, N.; El-Nahass, M.M. Enhancement of optical absorption and dispersion characteristics of nanocrystalline In_2Se_3 films: Impact of γ-ray irradiation. *Journal of Materials Science: Materials in Electronics* 2023, 34, 382. https://doi.org/10.1007/s10854-022-09776-4.
9. Moutaabbid, A.; Bernède, J.C.; Pouzet, J.; et al. Properties of photoconductive In_2Se_3 thin films, crystallized by post-deposition heat treatment in nitrogen atmosphere. *Applied Surface Science* 1999, 151(3-4), 171 – 176. https://doi.org/10.1016/S0169-4332(99)00300-1.
10. Feng, W.; Gao, F.; Hu, Y.; Dai, M.; Liu, H.; Wang, L.; Hu, P. Phase-Engineering-Driven Enhanced Electronic and Optoelectronic Performance of Multilayer In_2Se_3 Nanosheets. *ACS Applied Materials & Interfaces* 2018, 10 (33), 27584 – 27588. https://doi.org/10.1021/acsami.8b10194.
11. Sosa, J.F.T.; Hernández de la Luz, J.Á.D.; Hernández, O.L.; Diaz, G.J.; Salazar, P.L. Structural, morphological, and optical characterization of indium selenide (In_2Se_3) obtained by mechanical alloying. *Materials Research Express* 2025, 12, 015902. https://doi.org/10.1088/2053-1591/ada1a9.
12. Ward, L.; Agrawal, A.; Choudhary, A.; Wolverton, C. A general-purpose machine learning framework

for predicting properties of inorganic materials. *npj Computational Materials* 2016, 2, 16028.

13. Butler, K.T.; Davies, D.W.; Cartwright, H.; Isayev, O.; Walsh, A. Machine learning for molecular and materials science. *Nature* 2018, 559, 547–555. https://doi.org/10.1038/s41586-018-0337-2
14. Xie, T.; Grossman, J.C. Crystal graph convolutional neural networks for an accurate and interpretable prediction of material properties. *Physical Review Letters* 2018, 120, 145301. https://doi.org/10.1103/PhysRevLett.120.145301
15. Agrawal, A.; Choudhary, A. Perspective: Materials informatics and big data: Realization of the "fourth paradigm" of science in materials science. *APL Materials* 2016, 4, 053208. https://doi.org/10.1063/1.4946894
16. Li, W.; Cai, X.-F.; Valdes, N.; Wang, T.; Shafarman, W.; Wei, S.-H.; Janotti, A. In_2Se_3, In_2Te_3, and $In_2(Se,Te)_3$ alloys as photovoltaic materials. *The Journal of Physical Chemistry Letters* 2022, 13(51), 12026–12031. https://doi.org/10.1021/acs.jpclett.2c02975
17. Sharma, R.; Sharma, S.; Kumar, P.; Asokan, K.; Thangaraj, R.; Mian, M. Analysis of electrical conduction phenomena in highly photosensitive amorphous $In_xSb_{20-x}Ag_{10}Se_{70}$ ($0 \leq x \leq 20$) chalcogenide films. *Journal of Non-Crystalline Solids* 2017, 472, 70–74. https://doi.org/10.1016/j.jnoncrysol.2017.07.022
18. Marsillac, S.; Bernède, J.C.; Emziane, M.; Wery, J.; Faulques, E.; Le Ray, P. Properties of photoconductive In_2Se_3 thin films, crystallized by post-deposition heat treatment in nitrogen atmosphere. *Applied Surface Science* 1999, 151(3-4), 171–179. https://doi.org/10.1016/S0169-4332(99)00300-1
19. Breiman, L. Random forests. *Machine Learning* 2001, 45, 5–32. https://doi.org/10.1023/A:1010933404324
20. Hossain, J.; Julkarnain, M.; Sharif, K.S.; Khan, K.A. Preparation and properties of indium selenide (InSe) thin films for selective surface applications. *Journal of Physical Science and Application* 2011, 1, 37–42. https://doi.org/10.17265/2159-5348/2011.01.004
21. Hossain, J.; Julkarnain, M.; Mondal, B.K.; Newaz, M.A.; Khan, K.A. Unveiling the electrical and thermoelectric properties of highly degenerate indium selenide thin films: Indication of In_3Se_4 phase. *Materials Research Express* 2019, 6, 126421. https://doi.org/10.1088/2053-1591/ab5ac1
22. Zhu, X.; Liu, X.; Zheng, Q.; Wang, H.; Zhang, M.; Pan, X.; Tang, M.; Jin, M. Effects of sputtering pressure and annealing temperature on the characteristics of indium selenide thin films. *Materials Research Express* 2023, 10(10), 106403. https://doi.org/10.1088/2053-1591/ad02e2
23. Yudasaka, M.; Matsuoka, T.; Nakanishi, K. Indium selenide film formation by double-source evaporation of indium and selenium. *Thin Solid Films* 1987, 146, 65–73. https://doi.org/10.1016/0040-6090(87)90340-3
24. Yoo, M.H.; Park, Y.S.; Kim, N.H. Amorphous indium selenide thin films prepared by RF sputtering: Thickness-induced characteristic. *Journal of Nanoscience and Nanotechnology* 2016, 16, 5128 – 5132. https://doi.org/10.1166/jnn.2016.12207
25. Sreekumar, R.; Sajeesh, T.H.; Abe, T.; Kashiwaba, Y.; Sudha Kartha, C.; Vijayakumar, K.P. Influence of indium concentration and growth temperature on the structural and optoelectronic properties of indium selenide thin films. *physica status solidi (b)* 2013, 250(1), 95–102. https://doi.org/10.1002/pssb.201248268
26. Ateş, A.; Astam, A.; Kundakçı, M.; Yıldırım, M. Characteristic properties of indium selenide thin films grown by the successive ionic layer adsorption and reaction method. *Journal of Optoelectronics and Advanced Materials* 2009, 11(5), 644–648. https://joam.inoe.ro/articles/characteristic-properties-of-indium-selenide-thin-films-grown-by-the-successive-ionic-layer-adsorption-and-reaction-method/fulltext
27. Boolchandani, S.; Srivastava, S.; Vijay, Y.K. Preparation of InSe thin films by thermal evaporation method and their characterization. *Journal of Nanotechnology* 2018, 2018(1), 9380573. https://doi.org/10.1155/2018/9380573

28. Eji, M.O.; Sakib, M.S.H.; Corbett, J.P. Work function mapping across a-In_2Se_3 to α-In_2Se_3 to γ-InSe in RF-sputtered thin films. *arXiv* 2025, arXiv:2510.08767. https://doi.org/10.48550/arXiv.2510.08767
29. Fedyanina, M.E.; Pestova, V.B.; Pepelyaev, D.; Lebedeva, Y.S.; Babich, A.; Smayev, M.; Romashkin, A.V.; Nesterov, S.I.; Kozyukhin, S.A. Thermal and laser crystallization of InSe thin films formed by vacuum thermal evaporation. *Physics of Complex Systems* 2025, 6(2), 93 – 103. https://doi.org/10.33910/2687-153x-2025-6-2-93-103
30. Salman, S.H.; Ali, S.M.; Ahmed, G.S. Effect of annealing on structural and optical properties of indium selenide thin films prepared by vacuum thermal evaporation. *Journal of Physics: Conference Series* 2021, 1879, 032058. https://doi.org/10.1088/1742-6596/1879/3/032058
31. Yan, X.; Wu, X.; Fang, Y.; Zhang, S.; Chen, W.; Yao, C.; Wang, Y.; Zhang, X.; Song, Y. Morphological and nonlinear optical properties of Al: InSe thin films. *Optical Materials Express* 2019, 9(7), 2955 – 2963. https://doi.org/10.1364/OME.9.002955
32. Islam, M.A.; Alam, M.A.; Nuruzzaman, M.; Julkarnain, M.; Khan, K.A. Comparison of morphological, electrical and optical properties of as-deposited and annealed InSe thin films. *International Journal of Engineering Research and Applications* 2015, 5, 104 – 108. https://www.ijera.com/papers/Vol5_issue4/Part%20-%207/Q50407104108.pdf
33. Mondal, B.K.; Mostaque, S.K.; Islam, M.A.; Hossain, J. Stress-induced phase-alteration in solution processed indium selenide thin films during annealing. *RSC Advances* 2021, 11(23), 13751 – 13762. https://doi.org/10.1039/d1ra01403j
34. Raval, A.V.; Saini, L.K.; Shah, D.V.; Patel, S.K. Synthesis and characterization of indium selenide thin films for solar cell application. *AIP Conference Proceedings* 2020, 2220(1), 090029. https://doi.org/10.1063/5.0001309
35. Kavitha, B.; Dhanam, M. Study on InSe thin film prepared in the journey of $Cu(In_{1-x}Al_x)Se_2$ thin films. *Journal of Ovonic Research* 2010, 6(2), 75–80. https://www.chalcogen.ro/75_Kavitha.pdf
36. Emir, C.; Tataroglu, A.; Coşkun, E.; Ocak, S. B. Structural and Optical Properties of Interfacial InSe Thin Film. *ACS Omega* 2024, 9(7), 7588–7596. https://doi.org/10.1021/acsomega.3c06600
37. Tauc, J.; Grigorovici, R.; Vancu, A. Optical properties and electronic structure of amorphous germanium. *Physica Status Solidi B* 1966, 15, 627–637. https://doi.org/10.1002/pssb.19660150224